

An SI-traceable multilateration coordinate measurement system with half the uncertainty of a laser tracker

Joffray Guillory, Daniel Truong, Jean-Pierre Wallerand, Claes-Göran Svantesson, Magnus Herbertsson, Sten Bergstrand

▶ **To cite this version:**

Joffray Guillory, Daniel Truong, Jean-Pierre Wallerand, Claes-Göran Svantesson, Magnus Herbertsson, et al.. An SI-traceable multilateration coordinate measurement system with half the uncertainty of a laser tracker. Measurement Science and Technology, 2023, 34 (6), pp.1-13. 10.1088/1361-6501/acc26a . hal-04086635

HAL Id: hal-04086635
https://cnam.hal.science/hal-04086635

Submitted on 2 May 2023

HAL is a multi-disciplinary open access archive for the deposit and dissemination of scientific research documents, whether they are published or not. The documents may come from teaching and research institutions in France or abroad, or from public or private research centers.

L'archive ouverte pluridisciplinaire **HAL**, est destinée au dépôt et à la diffusion de documents scientifiques de niveau recherche, publiés ou non, émanant des établissements d'enseignement et de recherche français ou étrangers, des laboratoires publics ou privés.



Distributed under a Creative Commons Attribution 4.0 International License

Measurement Science and Technology

PAPER • **OPEN ACCESS**

An SI-traceable multilateration coordinate measurement system with half the uncertainty of a laser tracker

To cite this article: Joffray Guillory *et al* 2023 *Meas. Sci. Technol.* **34** 065016

View the article online for updates and enhancements.

You may also like

- Recent developments on an interferometric multilateration measurement system for large volume coordinate metrology
Eva Katharina Rafeld, Nils Koppert, Matthias Franke et al.
- Influence of high precision telescopic instrument characterization on multilateration points accuracy
S Aguado, F J Brosed, R Acero et al.
- Accuracy evaluation of geometric error calibration using a laser tracer via a formulaic approach
Hongdong Cong, Jun Zha, Linhui Li et al.

This content was downloaded from IP address 163.173.88.109 on 02/05/2023 at 11:00

OPEN ACCESS
IOP Publishing
Measurement Science and Technology
Meas. Sci. Technol. **34** (2023) 065016 (13pp)
https://doi.org/10.1088/1361-6501/acc26a

An SI-traceable multilateration coordinate measurement system with half the uncertainty of a laser tracker

Joffray Guillory[1,*], Daniel Truong[1], Jean-Pierre Wallerand[1], Claes-Göran Svantesson[2], Magnus Herbertsson[2] and Sten Bergstrand[2]

[1] Laboratoire Commun de Métrologie LNE-Cnam (LCM), Conservatoire National des Arts et Métiers (Cnam), 1 rue Gaston Boissier, 75015 Paris, France
[2] Department of Measurement Science and Technology, Research Institutes of Sweden (RISE), Box 857, 501 15 Borås, Sweden

E-mail: joffray.guillory@cnam.fr

Received 2 December 2022, revised 27 February 2023
Accepted for publication 8 March 2023
Published 23 March 2023

Abstract

We have validated the performance of a prototype coordinate measurement system based on multilateration by comparing it to a laser tracker, i.e. a well-proven instrument widely used in the industry. After establishing the uncertainty budget of the different systems, we performed position measurements with both instruments on common targets. Using the estimated uncertainties associated with the measurements, we found that the multilateration system provided lower position uncertainties than the laser tracker: on average 18 µm versus 33 µm for distances up to 12 m. The uncertainties represented by confidence ellipsoids are compatible between the two systems: for confidence regions of 95% probability, they overlap as expected, i.e. in 94% of the cases. We also measured the length of a 0.8 m long reference scale bar with the multilateration system at an error of only 2 µm. This cross-comparison is a new and key step in the characterization of this SI-traceable multilateration system.

Keywords: coordinate measurement system, multilateration, laser tracker, large volume metrology

(Some figures may appear in colour only in the online journal)

1. Introduction

Large volume metrology, i.e. the metrology for the dimensional measurements of large structures of several meters in size, covers a large number of industrial and research applications [1]. As examples, we cite assembly tolerances of aircraft wings that must be less than 0.3 mm [2] and the alignment requirements for particle accelerators, which are on the order of a few tens of micrometers over distances of a hundred meters [3]. Thus, to produce, assemble, or characterize these large parts and systems, accurate coordinate measuring systems such as large coordinate measuring machines, laser trackers, or multilateration systems [1, 4] are required.

In this context, a multilateration system with metrological traceability to the realization of the SI meter has been developed by Cnam [5–7]. This system has already been used for the reference point determination of a radio telescope at the geodetic observatory of Wettzell [8] as well as for the measurement of the movements of a six-axis industrial robot [9]. The purpose of the current study is to validate the performances of this multilateration system through comparisons with external references: a laser tracker and a scale bar. The comparison in this case means to measure the same points in space with

* Author to whom any correspondence should be addressed.

Original content from this work may be used under the terms of the Creative Commons Attribution 4.0 licence. Any further distribution of this work must maintain attribution to the author(s) and the title of the work, journal citation and DOI.

© 2023 The Author(s). Published by IOP Publishing Ltd

two different systems, quantify the differences between these two measurements, and check whether the uncertainties of the two instruments are compatible. These cross-comparisons are a new and key step for the characterization of this prototype of multilateration system, a crucial step that was not realized until now.

This paper is organized as follows. The sections from 2 to 4 present, successively, the multilateration system, the laser tracker, and the common target used for the comparison. In section 5, the uncertainty budgets of the two coordinate measurement systems are established. After that, the experimental setup used for the comparison is described in section 6. The workshop where the measurements took place is thus presented and the position of the targets are defined. In section 7, the experimental protocol of the comparison is detailed. Then, the experimental results are presented in section 8: the performances of the two instruments are evaluated and the measured positions and their uncertainties are compared. Lastly, in section 9, the multilateration system performance is evaluated using a scale bar.

2. The multilateration system

Multilateration is a technique for determining the position of a target T in space by measuring the distances between this target and known positions, corresponding in our case to measurement heads. From a geometric point of view, the position of T can be defined as the intersection of spheres centered at the measurement heads and of radii equal to the measured distances. In practice, the distances are determined by an absolute distance meter (ADM) and they are affected by zero-mean additive Gaussian noises. The coordinates of T are therefore rather determined by minimizing the following non-linear residual function:

$$\text{residual function} = \sum_{i=1}^{m} \left(d_i\left(x_T, y_T, z_T\right) + o_i - \|H_i - T\|\ \right)^2 \tag{1}$$

where $\|.\|$ denotes the Euclidian norm of a vector and $d_i(x_T,y_T,z_T)$ are the distances measured between the m measurement heads H_i and T. In practice, to solve the multilateration problem of formula (1), the number of heads should be at least equal to 4. The variables o_i are the instrument offsets of the heads, i.e. additive constants corresponding to the distances between the electro-optic origin of the ADM and the location of the heads.

The multilateration system characterized in this study adopts a self-calibration method[3]. This means that the coordinates of the measurement heads H_i and their instrument offset o_i do not need to be known since they are determined automatically by the algorithm. This is possible as soon as more than nine targets are measured, which results in a system of equations with more observations than unknowns. In that case, formula (2) shows how the coordinates of the heads H_i and targets T_j are estimated by non-linear least squares:

$$\text{residual function} = \sum_{\substack{i=1\ldots m \\ j=1\ldots n}} \left(\left(d_i\left(x_{T_j}, y_{T_j}, z_{T_j}\right) + o_i\right)^2 - \|H_i - T_j\|^2\right)^2 \tag{2}$$

with $m \geqslant 4$ for the measurement heads and $n \geqslant 10$ for the targets.

In summary, a multilateration system is a coordinate measurement system using only distance information for determination of three-dimensional positions. However, such a system is complex to implement since it requires the installation of several measurement heads. In our case, the system, presented in figure 1, is composed of a common ADM and of four measurement heads.

The principle of our in-house developed ADM is based on the measurement of the phase shift φ of a light modulated in intensity by a radio-frequency (RF) carrier f_{RF} at 5 GHz and propagated up to a retroreflective target. The measured distance d, proportional to the phase accumulated during this round trip, is therefore equal to:

$$d = \tfrac{1}{2} \times \left(\tfrac{\varphi}{2\pi} + N\right) \times \tfrac{c}{n_{\mathrm{air}} \times f_{\mathrm{RF}}} \tag{3}$$

where c is the speed of light in vacuum, n_{air} the air group refractive index through which the optical beam is propagated, and N an integer number corresponding to the number of synthetic wavelengths $\Lambda = c/(n_{\mathrm{air}} \times f_{RF})$ within the distance to be measured. In practice, N is determined by a set of measurements at different RF carriers.

One of the features of this ADM is its fiber-optic design based on optoelectronics components at 1550 nm, components from the telecommunication world, affordable and available in large quantities. The telemetric signal can thus be distributed through a fiber network before being emitted in free space in direction of a target by one of the measurement heads. For instance, the signal coming from the common ADM is shared between the four heads thanks to an optical switch. However, this approach also presents disadvantages since the four distance measurements to be performed for a given target are realized one after the other, in a time multiplex, which increases the measuring time and limits the measurements to static targets.

In this system, the measurement heads play both the role of a collimating system to propagate the optical beam over several tens of meters, and of an aiming system thanks to gimbal mechanisms for rotation of the laser beam in every direction of space around an invariant point as described in [5].

[3] In the literature, the term 'self-calibration' is generally used for such a system [21–23]. We therefore retain this term to qualify our system, even though in metrology the term 'calibration' refers to a measurement standard. In fact [24], talks about adjustment of a measuring system, the term 'self-adjustment' should be recommended instead.

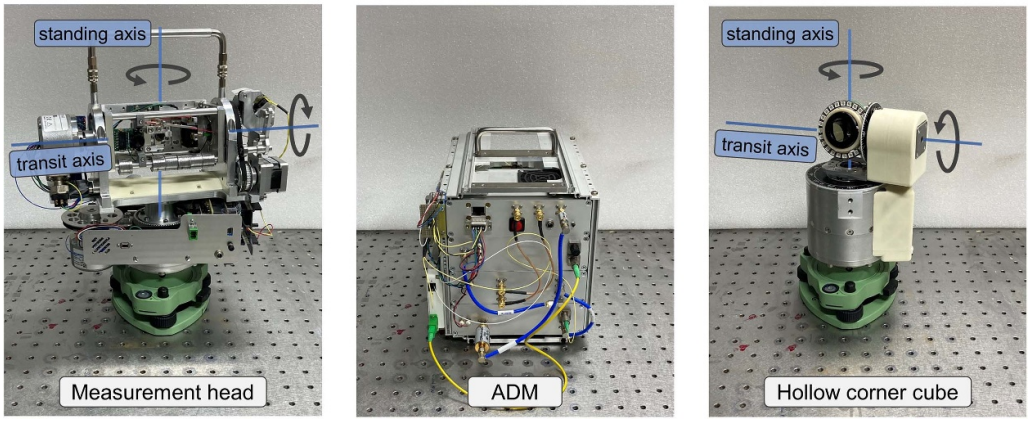


Figure 1. Prototype of a multilateration system composed of a shared absolute distance meter (ADM) visible in the middle, four measurement heads (from H_A to H_D) with H_c visible on the left, and a target visible on the right.

This multilateration system has been studied with a consistent metrological approach in [6]. For a distance measurement, the uncertainty contribution of the telemetric system is 2.1 µm (for a coverage factor $k = 1$, i.e. a confidence level of 68%) and that of a measurement head is 1.4 µm ($k = 1$). The latter is due to misalignments in its gimbal mechanism. This leads at the end to an uncertainty of 2.5 µm ($k = 1$). This value, validated by a comparison with an interferometric bench up to 35 m [7], does not depend on the measured distance.

This system can be used with two kinds of retroreflectors: hollow corner cube reflectors (CCR) [6] suitable for long-distance measurements (successfully tested up to 140 m), or glass spheres of refractive index 2 [7] (for distances up to 20 m). While the spheres induce high optical losses due to lower reflectivity and beam deflection at their output, they may be preferred since they offer a visibility from any angle[4] and are light weight.

3. The laser tracker

A laser tracker determines the position of a target in a spherical coordinate system by measuring the distance and the angles to the target. The distance to a target can be measured by an interferometer (IFM) or an ADM. The two orthogonal angles, the azimuth θ and the elevation ϕ, are measured by two angular encoders mounted along the mechanical axes of the gimbal mechanism of the laser tracker.

The laser trackers are a well-proven technology. In this study, a Leica AT960-LR from Hexagon and provided by RISE was used. Its performance as described in [10] on the basis of the ASME B89.4.19 standard, depends on two different contributions: the distance accuracy, $\pm 0.4\ \mu m + 0.3\ \mu m\ m^{-1}$ for the IFM mode or $\pm 10\ \mu m$ for the ADM one, and the angular accuracy, $\pm 15\ \mu m + 6\ \mu m\ m^{-1}$. These specifications are reported as maximum permissible errors (MPE), but they can also be expressed as typical values by taking half the MPE as result. In this paper, it has been considered that these typical values are the uncertainties for a coverage factor $k = 1$.

Expressed as a single number, the uncertainty σ_{pos} on a target position is calculated as follows[5]:

$$\sigma_{pos} = \sqrt{{\sigma_{ADM}}^2 + {\sigma_\theta}^2 + {\sigma_\phi}^2} \quad . \tag{4}$$

For instance, at a distance of 5 m, this corresponds to a MPE of 64 µm, or 32 µm when expressed as an uncertainty at $k = 1$. The main limitation comes from the angle measurements, so at the end, there is not a big difference in terms of uncertainty between the IFM and ADM modes. However, the IFM mode is capable of high-speed measurements and generally preferred for continuous measurements of dynamic objects, while the ADM mode is more practical for static measurements since it allows the beam to be broken, and so interruptions in a series of measurements. Thus, in the case of this comparison between the multilateration system and the laser tracker, the ADM mode has been adopted.

Contrary to a multilateration system, a laser tracker does not need to measure a large number of targets before determining their positions. The coordinates of a target are known directly, without the application of an onerous algorithm. However, the laser trackers are sensitive to temperature gradients, a situation that can be seen outdoors or in harsh industrial environments such as a workshop without air conditioning. These gradients can induce beam deflections, and so errors in the angle measurements of the laser tracker, which can lead in some cases to position errors of several tens of micrometers as reported in [11, 12]. Thus, for certain operations, the multilateration technique is more suitable as the length measurements are less susceptible to beam refraction than are the angular measurements: the knowledge of the angles is no longer necessary, only the distance data are required.

[4] This remains theoretical because in practice the spheres need a support. For example, they can be glued on a steel rod.

[5] This is a first calculation of the uncertainty σ_{pos}. Additional contributions can be considered as discussed subsequently in this paper, for example contributions from the air refractive index or the target.

The Leica AT960-LR is compatible with two kinds of retroreflectors, hollow CCRs or cat eyes. The CCRs allow measurements up to 80 m for this laser tracker, while the cat eyes are suitable up to 18 m with an acceptance angle for the laser beam of ±75 degrees.

4. The common target

To perform the comparison between the multilateration system and the reference laser tracker, a common target has been used. This avoids adding new sources of errors related to the geometric corrections required to compare two distinct targets.

The common target, depicted in figure 1 and characterized in [5], is a hollow corner cube with aluminum coating. It is mounted on a motorized gimbal mechanism developed by Cnam in order to be able to orientate itself towards any coordinate measurement instrument. The mechanical imperfections related to the different angular orientations of this rotating reflector induces errors in the measured distances, which are characterized by a Gaussian distribution of standard deviation 3.9 µm ($k = 1$). This uncertainty contribution, $\sigma_{\text{reflector}}$, should be included in the uncertainty budget of the distances measured by the ADM of the laser tracker and the ADM of the multilateration system.

For the comparison between the two coordinate measurement instruments, several target positions have been tested. In practice, a single target was used and moved from one position to another. Each position is related to a Leica tribrach, i.e. an adapter able to host a target on a Leica carrier.

5. Uncertainty budget of both systems

The table 1 shows a summary of the uncertainties of the two coordinate measurement systems, some of which have been presented in the previous sections.

In table 1, n_{air}, which allows to deduce a mechanical distance from an optical path, is also taken into account. The latter, usually calculated using the semi-empirical Edlén's equation [13] or similar updated formulas like Bönsch and Potulski [14], depends on the air temperature, the atmospheric pressure, the partial pressure of water vapor, and the CO_2 content. The main contributions come from the air temperature with a factor of −0.95 µm/(m × °C) and from the atmospheric pressure with a factor of 0.27 µm/(m × hPa). In practice, these environmental parameters are measured using local sensors. It has to be noted that the air refractive index also depends on the vacuum optical wavelength, 795 nm for the laser tracker (ADM mode) and 1550 nm for the multilateration system, but this parameter does not have a large impact compared to the environmental contributions reported in table 2.

Assuming that the impact of the air refractive index can be neglected, and knowing that the uncertainties related to the ADM and the common target are independent Gaussian-distributed contributions, the uncertainty on a distance measurement is equal to 6.3 µm for the laser tracker and 4.7 µm for the multilateration system ($k = 1$).

As shown in table 1, it is easy to determine the uncertainty on a target position measured by the laser tracker: it is equal to the square root of the sum of the variances of three independent sources of error. On the contrary, this is more complex for a target position measured by the multilateration system since this partly depends on the algorithm that allows to move from distance data to position values. In this process, the geometry of the system, i.e. the positions of the targets relatively to the four measurement heads, plays an important role on the uncertainties. For instance, the final uncertainty on a measured position, when expressed as a single number (see below in formula (5)), is at least 1.5 times the uncertainty of the measured distances for an ideal arrangement [15].

The uncertainties on the positions determined by multilateration have been assessed as performed in [16]. In summary, once the coordinates H_i and T_j have been estimated by the multilateration algorithm with self-calibration, each head is processed independently to evaluate their position uncertainties. For this purpose, the partial derivatives of the distances $\| H_i — T_j \|$ with respect to the coordinates of a studied head are calculated at the coordinates of that head. The resulting Jacobian matrices, one per head, describe how small changes in the coordinates of a head will change the distances derived from that position. It is then possible to find the covariance matrices of the head positions by a simple calculation as explained in [17]. With this first approximation, the multilateration problem becomes one where the head positions are known, but affected by zero-mean additive Gaussian noises of known covariance. Such a problem is then solved by applying the solution presented in [18]. In this way, the covariance matrix of each target position T_j is obtained.

From these 3 × 3 covariance matrices, the uncertainty of each target is expressed by a single number as follows:

$$\sigma_{\text{pos}}(T_j) = \sqrt{\text{Trace}\left(\text{cov}\left(T_j\right)\right)} \tag{5}$$

where cov(T_j) is the covariance matrix of the target position j, and Trace is an operator that returns the sum of the diagonal elements of the covariance matrix.

The mathematical solution for the uncertainty assessment of the positions has been validated in [16] thanks to comparisons with experimental measurements and Monte–Carlo simulations. However, the proposed approach considered measurement head and target positions determined by self-calibration with instrument offsets known. In our case the instrument offsets are determined by self-calibration, which means that no analytical solution is available. Therefore, the estimated uncertainties are probably optimistic, i.e. slightly lower than the reality. The comparison performed in this paper will therefore quantify this point.

After the establishment of the uncertainty budget, the next section focuses on the workshop where the comparison between the two instruments took place in order to define the positions of the targets relative to the instruments, but also to detail the environmental conditions of the experiment.

Table 1. Summary of the uncertainties of the two instruments.

Parameters		Uncertainty at $k = 1$	
		Leica AT960-LR laser tracker	Cnam multilateration system
σ_{ADM}	ADM	5.0 µm	2.5 µm
$\sigma_{\text{reflector}}$	Common target	3.9 µm	3.9 µm
σ_{n}	Refractive index	Details in table 2	
σ_{distance}	Global distance uncertainty	$\sqrt{{\sigma_{\text{ADM}}}^2 + {\sigma_{\text{reflector}}}^2 + {\sigma_{\text{n}}}^2}$	
		>6.3 µm	>4.7 µm
σ_θ and σ_ϕ	Angles	7.5 µm + 3.0 µm m^{-1}	Not required
σ_{pos}	Data processing	$\sqrt{{\sigma_{\text{distance}}}^2 + {\sigma_\theta}^2 + {\sigma_\phi}^2}$	Depends on the target positions relative to the head positions

Table 2. Error sources in the air group refractive index determination based on Edlén's formula.

Parameters		Conditions	Contribution
σ_T	Temperature	Around $T = 20$ °C,	−0.95 µm/(m × °C)
σ_p	Pressure	$p = 1013.25$ hPa,	0.27 µm/(m × hPa)
σ_{RH}	Humidity	$RH = 50\%$ and	−0.09 µm m^{-1} for +10%
σ_x	CO_2 content	$x = 450$ ppm, for $\lambda = 1550$ nm	0.03 µm m^{-1} for +200 ppm

6. Experimental setup

The comparison between the multilateration system and the laser tracker was carried out on 1 February 2022 between 12:45 pm and 3:30 pm, i.e. for 2 h 45 min. The workshop where the experiment took place is depicted in figure 2: this was in a large volume of about 6.3 m (x) × 10.3 m (y) × 3.1 m (z), a room without air conditioning, but located in a basement where temperature variations remain small. For instance, and as shown in figure 3, the temperature, as measured by our most accurate sensor, changed by less than 0.5 °C during the comparison. However, from one sensor to another, i.e. from different locations in the room, we have observed concurrent temperature differences of up to 0.4 °C. The CO_2 content, not depicted in figure 3, was also recorded. It was equal to 530 ppm ± 80 ppm.

The laser tracker has its own sensor for air refractive index compensation. It has recorded temperatures increasing from 18.7 °C to 18.9 °C, relative humidities increasing from 48.5% to 50.7%, and pressures decreasing from 1018.3 hPa to 1017.0 hPa. The differences between these environmental parameters and those used by the multilateration system are relatively small. The one that has the most impact is the pressure, with discrepancy up to 1.5 hPa. Such an error on the atmospheric pressure induces an error of 4.5 µm for a measured distance of 10 m.

In the end, it seems relevant to consider a length dependent uncertainty σ_{n} of 0.6 µm m^{-1} for the distances measured with the laser tracker as well as those of the multilateration system. This corresponds to environmental uncertainties of 0.4 °C for the temperature, 1.5 hPa for the pressure, 5% for the humidity, and 80 ppm for the CO_2 content.

In this large volume, the measurement heads of the multilateration system have been placed as depicted in figures 2 and 4. They formed a tetrahedron with sides of length between 3.4 m for $\| H_{\text{B}}—H_{\text{C}} \|$ and 6.9 m for $\| H_{\text{A}}—H_{\text{D}} \|$. Their coordinates, in meter, are:

$$\begin{cases} H_{\text{A}} = [0.00, 0.04, 0.26] \\ H_{\text{B}} = [2.69, 0.27, 2.62] \\ H_{\text{C}} = [5.28, 0.00, 0.47] \\ H_{\text{D}} = [2.73, 6.25, 1.47] \end{cases}$$

This arrangement is quite far from an optimal configuration. Indeed, in a multilateration system, the uncertainties on the target coordinates depend on their positions relative to the locations of the measurement heads. For instance, to minimize the measurement errors, a solution consists in setting up the targets at the center of a regular tetrahedron as explained in [15]. Thus, in an ideal case, the measurement head H_{B} would have been located at twice its height.

The ideal position of the laser tracker would have been in the middle of the working volume, but we have opted for a position outside this space to avoid any beam occlusion for the multilateration system. Thus, the laser tracker is located at the following coordinates, in meter:

$$LT = [-0.62, 0.87, 1.49].$$

As shown in figures 2 and 4, 18 different target positions have been defined across the room. Most of them have been placed inside the volume formed by the four heads, but less favorable configurations for the uncertainties of the multilateration system have also been tested. For instance, the target position T_3 is located 4 m behind the measurement head H_{D}. At the end, the distances measured the laser tracker are up 9.5 m, and those measured by the multilateration system are up to 11.6 m. The related uncertainties on the measured distances are thus between 6.4 µm and 8.5 µm for the laser tracker and between 4.7 µm and 8.4 µm the multilateration system.

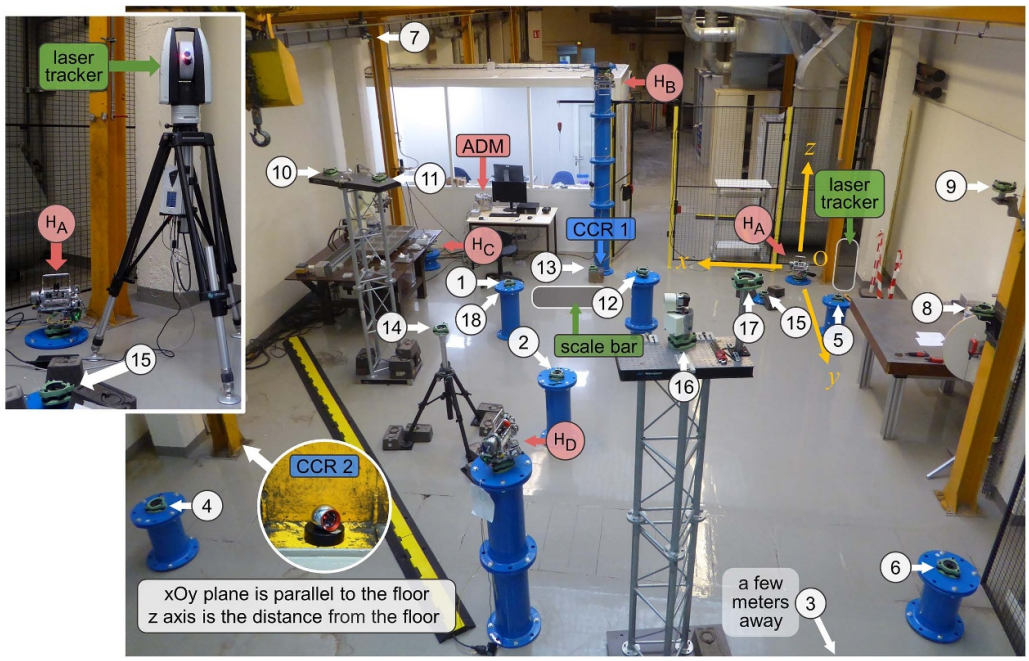


Figure 2. The experimental setup with the four measurement heads, from H_A to H_D, and the 18 target positions (the laser tracker, the scale bar, and the positions 3 and 18 are not visible in this photograph, but their position is reported), with a zoom on the left on the laser tracker Leica AT960-LR.

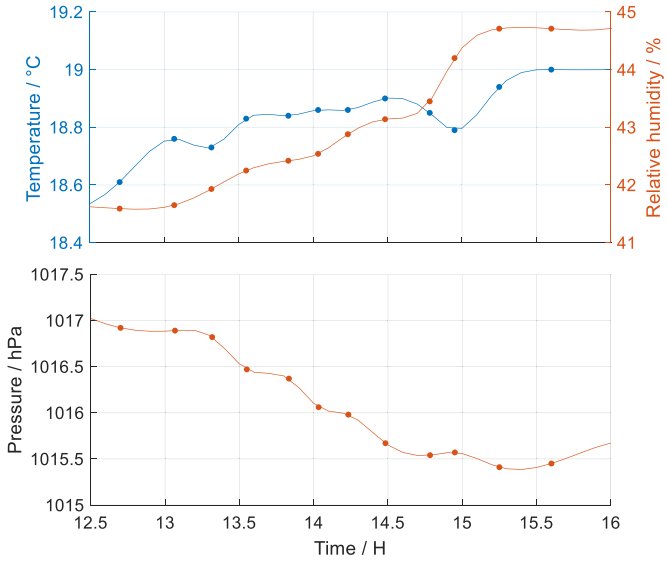


Figure 3. Environmental parameters recorded by a Vaisala PTU300 sensor and used by the multilateration system for air refractive index compensation. This sensor provides the temperature at ± 0.2 °C, the pressure at ± 0.25 hPa, and the relative humidity at $\pm 1\%$.

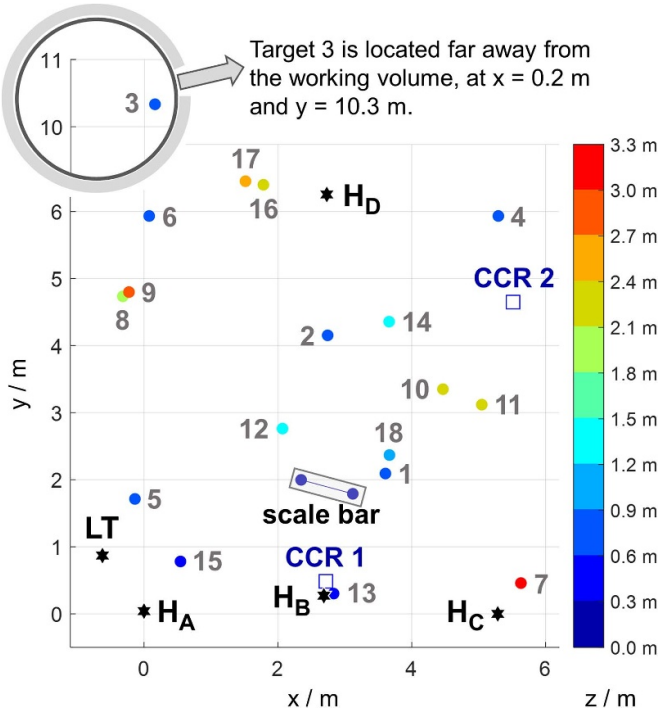


Figure 4. Top view of the experimental setup. The black stars represent the measurement devices, the points the targets, with the colors corresponding to their height, and the squares to reference targets used by the laser tracker.

7. Experimental protocol of the laser tracker comparison

The measurement protocol for the comparison of the two coordinate measurement systems comprised the following steps:

1. The target was placed in its initial position, on a leveled tribrach.
2. The four heads of the multilateration system started to aim at the target.
3. The retroreflector of the target was oriented in the direction of the head H_A, then the ADM of the multilateration

system measured the distance between this head and the target.
4. Step 3 was repeated for the measurement heads H_B, H_C and H_D.
5. The retroreflector was oriented in the direction of the laser tracker, and vice versa, then the laser tracker measured the distance and the angles that separated it from the target.
6. The target was moved into a new position.
7. Steps 2–6 were repeated for the 17 remaining target positions.

As explained above, the retroreflector was oriented in different directions at each position to aim at the different measurement heads of the multilateration system as well as the laser tracker. These changes of orientation of the retroreflector broke the optical beam of the laser tracker, which is why the ADM mode of the laser tracker was preferred for the distance measurements as explained in section 3.

Besides, the coordinates of a target measured by the laser tracker was the average of three successive position measurements, each of them being the average of two-face measurements. A two-face measurement consists in measuring a position from the front face of the laser tracker, then measuring it from its back face, which is achieved by changing the azimuth angle by 180°, then adjusting the elevation angle. In the end, the difference between three successive position measurements for a given coordinate can be up to 24 µm with an RMS value of 8 µm for all the targets. Lastly, a warm-up time of 4 h was applied to the laser tracker before the first measurement.

8. Experimental results

8.1. The multilateration system

The coordinates of the 18 targets, as determined by the multilateration system, are obtained after applying a multilateration algorithm with self-calibration, which consists in processing the 4×18 measured distances to minimize the residual function in formula (2). The differences between the distances measured by the telemetric system and those calculated from the obtained coordinates were used to quantify the quality of the multilateration results in figure 5.

These errors are lower than 4.3 µm with a global standard deviation of only 1.5 µm. The multilateration algorithm has therefore perfectly converged. This also shows that the assessed uncertainties between 4.7 µm and 8.4 µm may be too pessimistic.

8.2. The laser tracker

The measurement heads were installed on ductile cast iron pipes fixed to the ground to guarantee a high stability, whereas the laser tracker was installed on a tripod (see figure 2). The pipes were installed several months before the measurement campaign, and it is assumed that their position does not to drift during the few hours of the measurement. On the contrary, the tripod of the laser tracker was installed on the day of the measurement and may move over time. In order to monitor the laser tracker stability during the experiment, two additional CCRs were mounted close to the ground and measured every hour. Their position, visible in figures 2 and 4, are assumed to be fixed. Thus, as shown by the curves in figure 6, which represents the distances that separate the laser tracker from these reference CCRs, the laser tracker moves over time, up to 30 µm for CCR 1 during the comparison of 2 h and 45 min. Such a drift is problematic for the comparison since it is of the same order of magnitude as the assessed uncertainties.

The coordinates of these two reference CCRs were studied in detail to explain these distance drifts. We have identified a continuous rotation of the laser tracker around its z-axis of 0.82 µrad per hour, and a translation of the laser tracker of few micrometers per hour. The latter is visible by correcting only the continuous rotation, as shown in figure 7. In these curves, after fitting by regression lines, the residuals have standard deviations along the x, y and z axes of, respectively, 2.9 µm, 1.7 µm and 3.5 µm.

In practice, since the positions of the reference CCRs are assumed to be fixed, the coordinates of all the targets measured by the laser tracker have been corrected. However, no additional uncertainty was considered for these corrections.

8.3. The position uncertainties

The position uncertainties σ_{pos} of the 18 targets, noted σ_{LT} and σ_{MLT} to differentiate the laser tracker from the multilateration system, are presented in figure 8 in the form of single numbers. Those determined by the multilateration system are always lower than those measured by the laser tracker, with an average value of 18 µm versus 33 µm. For the positions measured by the laser tracker, their uncertainties increase with the measured distances by a factor of 4.2 µm m^{-1}. Thus, T_3 located at 9.5 m from the laser tracker, presents the highest uncertainty with a value of 52 µm. In the multilateration case, T_3 has again the highest uncertainty with a similar value of 51 µm, but this time due to a position largely outside the volume formed by the four measurement heads.

8.4. The comparison of the measured positions

In this part, the measurements performed by the multilateration system are compared with those performed by the commercial laser tracker to demonstrate that the in-house developed multilateration system works well and that its uncertainties have been properly assessed.

To compare the two sets of coordinates, the one obtained by the laser tracker with the one obtained by the multilateration system, a point-set registration using a Horn's quaternion-based algorithm [19] has been performed to express the different results in a unique system of coordinates. This consists in finding a translation vector t and a rotation matrix R that best match one collection of target coordinates to another one in a least squares sense:

$$residualfunction = \sum_{j=1}^{18} w(j) \times \left\| R \cdot T_{LT}(j) + t - T_{MLT}(j) \right\|^2 . \quad (6)$$

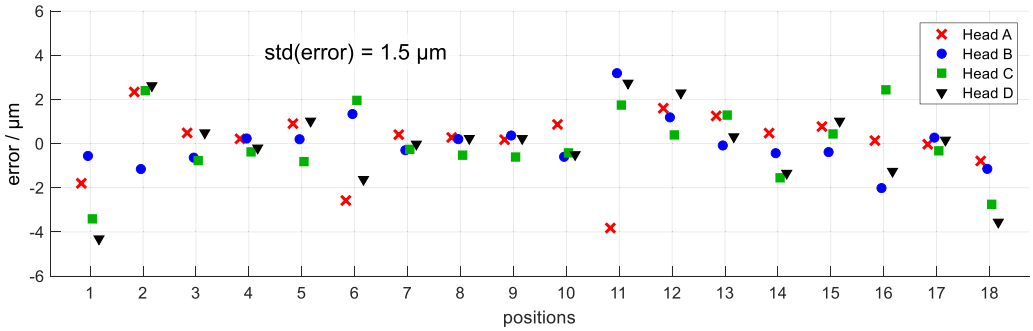


Figure 5. Difference between the 4 × 18 distances measured by the ADM and the distances deduced from the positions obtained by multilateration algorithm with self-calibration. The errors are colored according to the head having carried out the distance measurement.

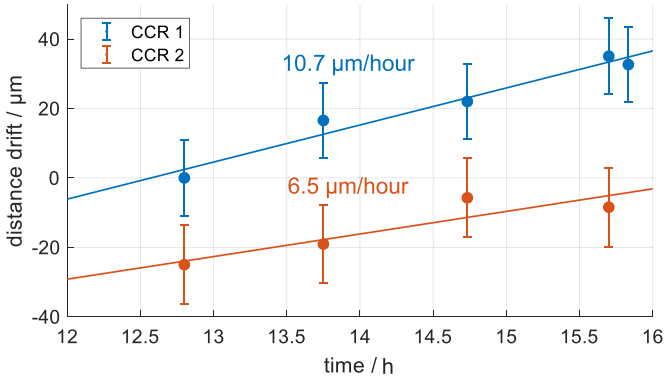


Figure 6. Drifts of the distances measured between the laser tracker and the two reference CCRs. CCR 1 is located at 3.6 m and CCR 2 at 7.3 m from the laser tracker.

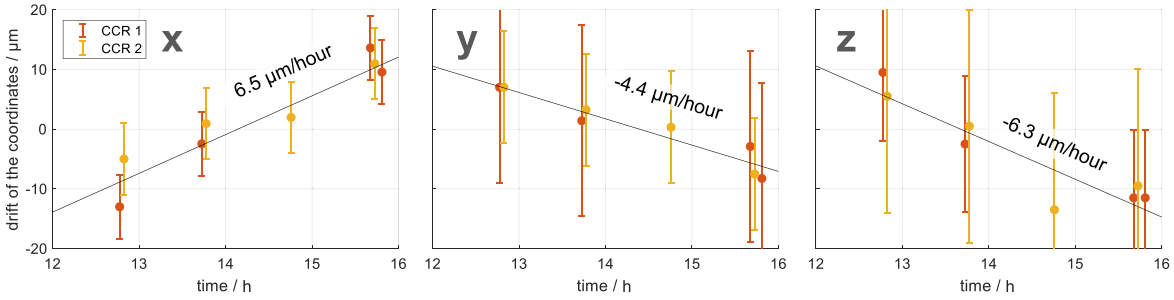


Figure 7. Drifts of the coordinates of the two reference CCRs after applying a rotation around the z-axis of the laser tracker.

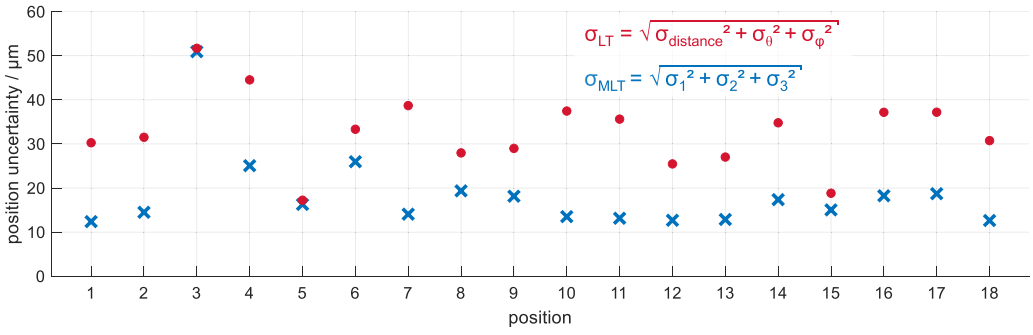


Figure 8. Uncertainties of the target positions measured by the two coordinate measurement systems.

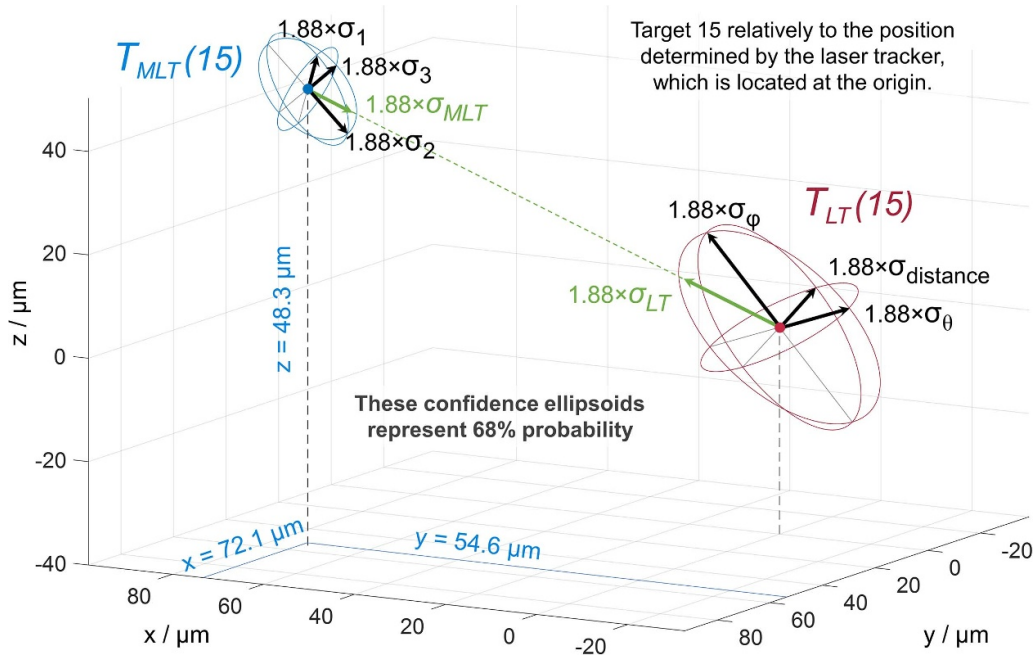


Figure 9. Three-dimensional view of the positions and uncertainties of T_{15}, which corresponds to the highest position differences between the laser tracker and the multilateration system. The perspective distorts the lengths, $1.88 \times \sigma_\phi = 1.88 \times \sigma_\varphi$.

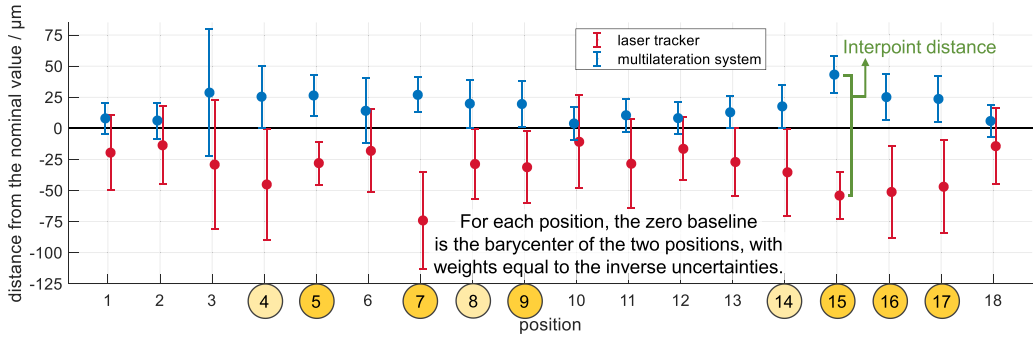


Figure 10. Interpoint distances between the positions measured by multilateration with self-calibration (in blue) and those determined by the laser tracker (in red). The seven positions circled in yellow do not overlap.

To carry out properly this adjustment, the position uncertainties have been considered by introducing the weights w. Thus, the positions with high uncertainties are not as well aligned as those with low uncertainties:

$$w(j) = \left(\frac{1}{\sigma_{\mathrm{LT}}(j)+\sigma_{\mathrm{MLT}}(j)}\right)^2 . \tag{7}$$

The uncertainties of the measured positions can be expressed by a single number, σ_{pos}, as shown in table 1 with the example of the laser tracker. However, it is more rigorous to consider the geometry of the uncertainties in three-dimensional space, which are defined by confidence ellipsoids. An example is shown in figure 9 for the case of T_{15}. For the positions measured by the laser tracker, T_{LT}, the axis of length $1.88 \times \sigma_{\mathrm{distance}}$ corresponds to the direction of the optical beam of the laser tracker. The two other axes, radial to the direction of the optical beam, correspond to the angle measurements. Their lengths are equal to $1.88 \times \sigma_\theta$ and $1.88 \times \sigma_\phi$, respectively. The factor 1.88 is due to the move from a one-dimensional to a trivariate error distribution [20]. For the positions measured by the multilateration system, T_{MLT}, the determination of their confidence ellipsoid results from the covariance matrices obtained by applying the mathematical solution presented in [16].

Thus, in formula (7), the uncertainty σ_{LT} is the uncertainty of T_{LT} with respect to T_{MLT}. This corresponds to the distance between the center of its confidence ellipsoid and the point of this ellipsoid in the direction of T_{MLT} as depicted in figure 9. The same method is done for the determination of σ_{MLT}.

Once the two sets of coordinates are expressed in a unique frame thanks to the weighted least squares detailed in formula (6), the results are compared. First, for each position, the distance between the point measured by the laser tracker and that point when it is measured by the multilateration system is depicted in figure 10, where the $k = 1$ uncertainty bars represent the values in figure 8. These distances are plotted relative

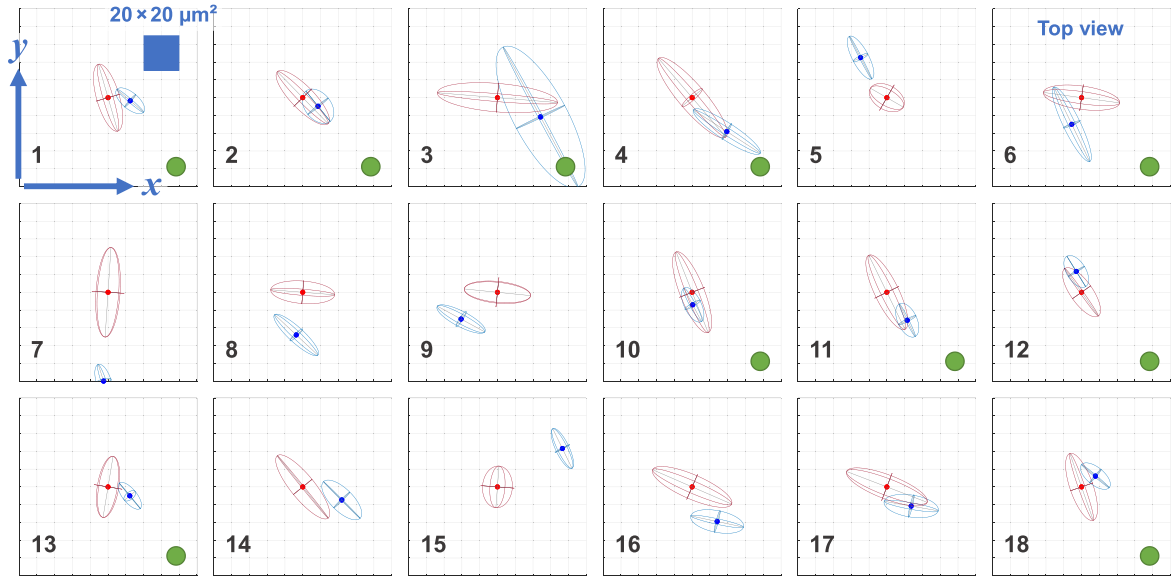


Figure 11. Top view (xOy plane) of the targets measured by the laser tracker in the center and in red, and the ones determined by multilateration around it in blue. The confidence ellipsoids represent confidence regions of 68% probability. Each figure corresponds to a 100 µm × 100 µm box, with grid lines every 10 µm.

to a zero baseline, which is the barycenter (i.e. weighted mean) of the two positions, with weights equal to the inverse of the uncertainties of each instruments.

The interpoint distances between the measurements of the laser tracker and those of the multilateration system are between 14 µm and 101 µm with an average value of 50 µm. First, it can be noted that the positions close to each other, like the positions 5 and 15, or 16 and 17, produce similar results. Then, the highest observed errors are obtained for the positions 7 and 15 with uncertainty bars distant of more than 48 µm. For position 7, installed at 3.0 m above the ground, i.e. the highest position of the setup, this can be explained by a location outside the volume formed by the measurement heads of the multilateration system. However, the observed errors are less understandable for the positions 15. The latter, like the position 5 which also appears inaccurate, is very close to the laser tracker, and therefore its uncertainty is low. It may be errors in the elevation angles of the laser tracker: positions 5 and 15 correspond to high values with, respectively, $-40.1°$ and $-45.5°$, while the other target positions have elevation angles between $-18°$ and $+18°$.

At the end, the uncertainty bars at $k = 1$ of the two sets of coordinates overlap for nine positions. Positions 4, 8, 14 are excluded from these positions, but for less than 1.3 µm. When considering uncertainty bars at $k = 2$ (not depicted here), only the positions 15 do not overlap. Thus, 50% and 94% of data points lie within, respectively, one and two standard deviations. This demonstrated that the uncertainties of the two systems are compatible for $k = 2$ since we should have obtained a percentage of 95%.

It is also possible to examine the results in three-dimensional space. In this case, the standard deviations of the differences in coordinates between the two systems are equal to 28.5 µm, 34.0 µm and 28.8 µm for, respectively, the x, y, and z axes. To better analyze this, figures 11 and 12 have been plotted. They represent, for each target, the coordinates determined by the multilateration system relatively to the position measured by the laser tracker, with confidence regions of 68% probability. For the presentation, we have chosen the laser tracker coordinates as the origin of the individual target reference frames.

When the results are observed in the xOz plane, the confidence ellipsoids of the two instruments overlap in most cases. More specifically, the z coordinates of the different target positions measured by the laser tracker and the multilateration system are very similar, only the positions 4, 15, 16 and 17 present differences higher than 44 µm when other are lower than 30 µm. In the xOy plane, the observed discrepancies are higher, especially for the y coordinates.

In three-dimensional space, ten positions over 18 have the confidence ellipsoids of the two coordinate measurement instruments that overlap, i.e. 56% of the positions have compatible confidence regions. This reveals that the three-dimensional representation can change a little the results, but we still do not reach the expected 68%. These 10 positions are marked by green dots in figures 11 and 12. A majority of them are located at the center of the tetrahedron formed by the four measurement heads as shown in figure 4. The results seem therefore to partly depend on the position of the targets relatively to the location of the heads of the multilateration system. For confidence regions of 95% probability, only the position 15 has confidence ellipsoids that do not overlap. In other words, 94% of the positions have compatible confidence regions, as expected.

At the end, the results in three-dimensional space shows that the confidence regions of 68% probability seem slightly undervalued. Firstly, with the small number of measured targets, it is difficult to verify accurately whether the uncertainties

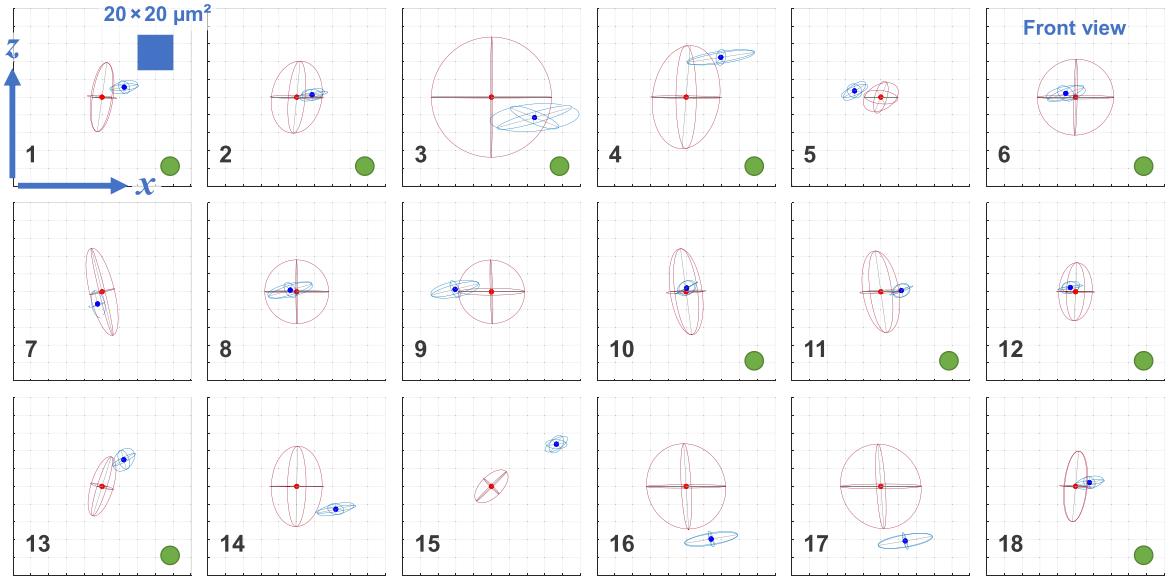


Figure 12. Front view (xOz plane) of the targets measured by the laser tracker in the center and in red, and the ones determined by multilateration around it in blue. The confidence ellipsoids represent confidence regions of 68% probability.



Figure 13. Photograph of the Leica scale bar, with on the left a SMR installed on the nest.

of the two instruments are compatible. Therefore, differences of a few percent can be explained in this way. Secondly, the position of the laser tracker drifted over time as pointed out in section 8.2. Corrections were made for the coordinates measured by the laser tracker, but no uncertainty was attributed to them. Thirdly, and as previously explained in section 5, the errors resulting from the determination of the instrument offsets by self-calibration was not taken into account. This point is probably the most important. Lastly, the point set registration algorithm probably also induces errors. So, there are additional uncertainty contributions that should have been considered, but these seem minor.

9. Comparison with the scale bar

Tocomplete the comparison, the length of a reference scale bar has also been measured by the multilateration system. This scale bar equipped with two nests is shown in figure 13. It has a nominal length of 800.169 mm ± 5 µm at 20 °C for a coverage factor $k = 2$. This value results from an interferometric calibration using the accompanied target, a spherically mounted retroreflector (SMR, which is a hollow CCR) of 1.5 inch diameter.

This new comparison has been realized 1 h after the measurements with the laser tracker, at 4:30 pm under a temperature of 19 °C, using a classical multilateration technique with the coordinates of the measurement heads and the instrument offsets determined previously. As depicted in figures 2 and 4, the scale bar has been positioned on the ground between the four heads. The used target was the 1.5 inch diameter SMR, oriented manually in the direction of the different measurement heads.

The interpoint distance between the two nests, when determined by the multilateration system, is equal to 800.166 mm ± 10 µm. The uncertainty on this interpoint distance has been calculated as the combined uncertainty of two independent positions. Let T_{19} and T_{20} be these two target positions. The uncertainty of T_{19} is equal to the distance between the center of its confidence ellipsoid and the point of this ellipsoid in the direction of T_{20}, and inversely for uncertainty of T_{20}.

$$\sigma\left(\|T_{19} - T_{20}\|\right) = \sqrt{\sigma_{T19(\text{with respect to } T20)}{}^2 + \sigma_{T20(\text{with respect to } T19)}{}^2} = 10\ \mu\text{m}. \quad (8)$$

At the end, the error between the measured distance and the nominal value is equal to only 2 µm. A length correction of 1.2×10^{-6} per kelvin was performed to take into account the thermal expansion coefficient of the scale bar made of Invar.

$$error = 800.166\ \text{mm} - 800.169\text{mm} \times \left(1 - 1.2 \cdot 10^{-6} K^{-1} \times 1\ K\right) = -0.002\ \text{mm} \quad (9)$$

The position measurements of the multilateration system are therefore compatible with the length of the scale bar.

10. Conclusion

A multilateration system with a metrological traceability to the SI meter has been developed. This is an alternative to the spherical measurement systems, such as laser trackers, to reduce the errors linked to angle measurements in difficult environments with for example temperature gradients. Indeed, a multilateration system only requires distance information for determination of three-dimensional positions.

This multilateration system is based on an absolute distance meter and four measurement heads. When used with a hollow corner cube as target, it allows distance measurements up to 140 m with an uncertainty of 4.7 µm in a controlled environment, i.e. when the air refractive index is well known.

To validate the performance of this system, it was compared with two external references: a laser tracker and a scale bar. This was done in a large volume of about 6.3 m × 10.3 m × 3.1 m, a workshop without air conditioning, but with a temperature stable within 0.5 °C over several hours. In this environment, an additional uncertainty contribution of 0.6 µm m^{-1} was considered on the distance measurements for the air refractive index correction.

Eighteen positions of a common target were measured for comparison with the laser tracker, then two more for determination of the length of a scale bar. The distance differences between the 18 first target positions measured by the laser tracker and those determined by multilateration are equal to 50 µm on average for distances up to 11.6 m. Then, for the two last target positions corresponding to the scale bar, the interpoint distance differs from the nominal value by only 2 µm. This demonstrates the proper functioning of the developed multilateration system.

The position uncertainties assessed for the multilateration system, when expressed as a single number, were between 11 µm and 51 µm, values 1.8 times lower on average than those obtained by the laser tracker. The uncertainties of the two instruments were quite compatible, even if the confidence regions of the positions determined by multilateration have been slightly undervalued. Indeed, the uncertainty contribution of the determination of the instrument offsets by self-calibration has not been taken into account.

Finally, in three-dimensional space, 56% of the measured positions have the confidence ellipsoids of the two systems that overlap, instead of the 68% probability represented by their confidence regions. However, as expected, this value reaches 94% for confidence regions of 95% probability. In this case, the impact of the errors resulting from the determination of the instrument offsets by self-calibration is likely to be negligible. Nevertheless, in the future, the instrument offsets will be determined in a different way, through additional calibration measurements, in order to take into account its contribution to the uncertainty.

Data availability statement

All data that support the findings of this study are included within the article (and any supplementary files).

Acknowledgments

This work was partially funded by Joint Research Project (JRP) 17IND03 LaVA, project that has received funding from the European Metrology Programme for Innovation and Research (EMPIR) co-financed by the Participating States and from the European Union's Horizon 2020 research and innovation programme.

ORCID iDs

Joffray Guillory https://orcid.org/0000-0002-0325-1695
Sten Bergstrand https://orcid.org/0000-0001-5203-5465

References

[1] Schmitt R H, Peterek M, Morse E, Knapp W, Galetto M, Härtig F, Goch G, Hughes B, Forbes A and Estler W T 2016 Advances in large-scale metrology—review and future trend *CIRP Ann.* **65** 643–65
[2] Martin O C, Wang Z, Helgosson P, Muelaner J E, Kayani A, Tomlinson D and Maropoulos P G 2011 Metrology enhanced tooling for aerospace (META): a live fixturing, wing box assembly case study *7th Int. Conf. on Digital Enterprise Technology (DET)* (*Athens, Greece*)
[3] Leão R J, Baldo C R, Reis M L C C and Trabanco J L A 2018 Engineering survey planning for the alignment of a particle accelerator: part I. Proposition of an assessment method *Meas. Sci. Technol.* **29** 034006
[4] Rafeld E K, Koppert N, Franke M, Keller F, Heißelmann D, Stein M and Kniel K 2022 Recent developments on an interferometric multilateration measurement system for large volume coordinate metrology *Meas. Sci. Technol.* **33** 035004
[5] Guillory J, Truong D and Wallerand J-P 2020 Assessment of the mechanical errors of a prototype of an optical multilateration system *Rev. Sci. Instrum.* **91** 025004
[6] Guillory J, Truong D and Wallerand J-P 2020 Uncertainty assessment of a prototype of multilateration coordinate measurement system *Precis. Eng.* **66** 496–506
[7] Guillory J, Truong D, Wallerand J-P and Alexandre C 2022 Absolute multilateration-based coordinate measurement system using retroreflecting glass spheres *Precis. Eng.* **73** 214–27
[8] Lösler M, Eschelbach C, Mähler S, Guillory J, Truong D, Wallerand J-P and Klügel T 2022 Operator-software impact

in local tie networks: case study at geodetic observatory Wettzell *Appl. Geomat.* (https://doi.org/10.1007/s12518-022-00477-5)

[9] Guillory J, Truong D, Wallerand J-P, El Ghazouali S, Vissière A and Nouira H 2021 Robot characterization based on a multilateration system with retroreflecting spheres n=2 as targets *3D Metrology Conf. (3DMC)*

[10] Hexagon website, datasheet Leica absolute tracker AT960 (available at: www.hexagonmi.com/products/laser-tracker-systems/leica-absolute-tracker-at960)

[11] Pérez Muñoz P, Albajez García J A and Santolaria Mazo J 2016 Analysis of the initial thermal stabilization and air turbulences effects on laser tracker measurements *J. Manuf. Syst.* **41** 277–86

[12] Robson S, MacDonald L, Kyle S, Boehm J and Shortis M R 2016 Optimized multi-camera systems for dimensional control in factory environments *Proc. Inst. Mech. Eng.* B **232** 1707–18

[13] Edlén B 1966 The refractive index of air *Metrologia* **2** 71–80

[14] Bönsch G and Potulski E 1998 Measurement of the refractive index of air and comparison with modified Edlén's formulae *Metrologia* **35** 133–9

[15] Lin Y and Zhang G 2003 The optimal arrangement of four laser tracking interferometers in 3D coordinate measuring system based on multi-lateration *Proc. Int. Symp. on Virtual Environments, Human-Computer Interfaces and Measurement Systems (VECIMS)* (*Lugano, Switzerland*) pp 138–43

[16] Guillory J, Truong D and Wallerand J-P 2022 Multilateration with self-calibration: uncertainty assessment, experimental measurements and Monte-Carlo simulations *Metrology* **2** 241–62

[17] Donaldson J R and Schnabel R B 1987 Computational experience with confidence regions and confidence intervals for nonlinear least squares *Technometrics* **29** 67–82

[18] Ma Z and Ho K C 2011 TOA localization in the presence of random sensor position errors *Proc. Int. Conf. on Acoustics, Speech and Signal Processing (ICASSP)* (*Prague, Czech Republic*)

[19] Jacobson M Absolute orientation—Horn's method *Matlab central file exchange* (available at: www.mathworks.com/matlabcentral/fileexchange/26186-absolute-orientation-horn-s-method)(Accessed January 2022)

[20] Mitchell J, Spence A, Hoang M and Free A 2003 Sensor fusion of laser trackers for use in large-scale precision metrology *Proc. of Photonics Technologies for Robotics, Automation, and Manufacturing* (*Providence, Rhode Island*)

[21] Zhuang H, Li B, Roth Z S and Xie X 1992 Self-calibration and mirror center offset elimination of a multi-beam laser tracking system *Robot. Auton. Syst.* **9** 255–69

[22] Campbell M and Hughes B 2016 A high-accuracy, self-calibrating and traceable coordinate measurement system *16th European Society for Precision Engineering and Nanotechnology (Euspen) Int. Conf. & Exhibition* (*Nottingham, United Kingdoms*)

[23] Nitsche J, Franke M, Haverkamp N and Heisselmann D 2021 Six-degree-of-freedom pose estimation with µm/µrad accuracy based on laser multilateration *J. Sens. Sens. Syst.* **10** 19–24

[24] Bureau International des Poids et Measures (BIPM) 2012 The international vocabulary of metrology—basic and general concepts and associated terms (VIM) 3rd edn *JCGM 200:2012* (available at: www.bipm.org/vim)